第 48 卷 第 9 期
2021 年 9 月

湖南大学学报（自然科学版）
Journal of Hunan University (Natural Sciences)

Vol. 48. No. 9.
September 2021

Large Scale LED-Modular-Based Solar Simulator and Calibration Method for PV-Module Characterization

Napat Watjanatepin, Patcharanan Sritanauthaikorn

Solar Energy Research Technology Transfer Center (SERTT), Faculty of Engineering and Architecture, Rajamangala University of Technology Suvarnabhumi, Nonthaburi, Thailand

Abstract: This study aims to design and construct a large-scale LED-based solar simulator by using a mix of the six colors of the LED modular system and to confirm the method of solar panel test under low radiation conditions with a simple calibration factor technique. The performance tests were executed on the characteristics of irradiance under IEC 60904-9 edition 2. The constructed prototype was applied for testing the I-V characteristic of the PV module under non STC. The LED module consisted of nine 50 W LEDs as the six specific wavelengths covering 400 nm – 1100 nm range. The twelve LED modules were suitable for an extended application as a large area solar simulator. The testing results showed that the spectral mismatch and the temporal instability were of class A+ and the non-uniformity was in class C. The average irradiance of solar simulator on the test plane of 152 cm × 96 cm was about 384 W/m^2. This proposed method was a practical alternative method to test the mono crystalline PV module under low radiation condition. The I-V characteristic of the mono crystalline PV module tested by the solar simulator prototype was reasonable, and the I-V characteristic could be plotted and estimated by using a calibration factor.

Keywords: LED module, large scale solar simulator, calibration factor, I-V characteristic.

用于光伏模块表征的大规模基于引领模块的太阳能模拟器和校准方法

摘要：本研究旨在通过混合使用引领模块化系统的六种颜色来设计和构建基于引领的大型太阳能模拟器，并通过简单的校准因子技术确认低辐射条件下的太阳能电池板测试方法。根据国际电工委员会 60904-9第2版对辐照度特性进行性能测试。构建的原型用于测试非STC下光伏组件的一世-伏特性。引领模块由九个 50 宽引领作为六个特定波长组成，涵盖 400纳米– 1100纳米范围。十二个引领模块适用于作为大面积太阳能模拟器的扩展应用。测试结果表明，光谱失配和时间不稳定性为一种+级，不均匀性为C级。太阳模拟器在152厘米×96厘米测试平面上的平均辐照度约为384瓦/平方米。该方法是在低辐射条件下测试单晶光伏组件的实用替代方法。太阳能模拟器样机测试的单晶光伏组件的一世-伏特性合理，可以使用校准因子绘制和估计一世-伏特性。

关键词：引领模块、大型太阳模拟器、校准系数、一世-伏特性。

1. Introduction

The utilization of a solar simulator as an artificial light source has been studied on performance and characteristic of the solar thermal devices and the photovoltaic (PV) applications. The solar simulator for PV applications is arranged in the terrestrial PV system AM1.5 global solar simulator. There are three solar simulators standards: (1) IEC 60904-9 [1], (2) JIS-C-8912 [29] and (3) ASTM E927-05 [30]. Several features and parameters of solar simulators are

Received: June 1, 2021 / Revised: June 6, 2021 / Accepted: July 28, 2021 / Published: September 30, 2021

About the authors:Associate Professor Napat Watjanatepin, Ms. Patcharanan Sritanauthaikorn, Solar Energy Research Technology Transfer Center (SERTT), Faculty of Engineering and Architecture, Rajamangala University of Technology Suvarnabhumi, Nonthaburi, Thailand

Corresponding authors Napat Watjanatepin, napat.w@rmutsb.ac.th; Patcharanan Sritanauthaikorn, patcharanan.s@rmutsb.ac.th

described according to these standards [1]. Most previous studies had developed the small-scale solar simulators on test plane of about 36 cm^2 to 360 cm^2. Some of these studies used a xenon-arc lamp, a halogen lamp, or a combination of an electrodeless sulfur lamp and a halogen lamp as the light source [2], [3].

Currently, the use of LED as the light source is advantageous due to the LEDs properties, such as high luminous efficacy, long operational life and ability to produce specific spectrums, including UV, visible and IR. For example, Novičkovas et al. [4] designed a solar simulator incorporating 4 different LEDs that could produce a spectrum with a range of 400–950 nm. Tavakoli et al. [5] reported the developed solar simulator with nineteen-colors of LEDs and achieved the ASTM and IEC in class A. Esen et al. [6] created the LED solar simulator by mixing blue, white and near-farred spectra of wavelengths of 730-940 nm to achieve a spectrum mismatch of class A. Some studies reported the design of LED solar simulators using 5 or 6 colors of LEDs which could offer in a spectrum of 400-1100 nm. Other studies revealed that the 11 color LEDs module provided a spectrum of 399 – 728 nm. The 14 color LEDs module resulted in a wavelength range of 350-1100 nm, and so on [7]-[14]. These previous studies indicated that using many LED colors (spectrum) could produce a spectrum of light imitating similar to the natural sunlight and being under class A standard. To make the light spectrum was followed: may be used the complex mathematical models, including design, creation, and control technologies.

To test the characteristics of a PV module, a large light area is required for the solar simulator. The large-scale solar simulator must have strong properties in spectral match, nonuniformity, and instability of irradiance in order to fit the standard. A large-scale solar simulator would typically use xenon lamps, metal halide lamps, halogen lamps, or LED mixed halogen lamps [15], [16]. However, these systems consume large amounts of power and radiate considerable heat loss [17]. Al-Ahmad et al. [18] created a new solar simulator design using an LED module; it is 32 cm × 9 cm in size and consists of 10 colors and 266 LED units installed on the multilayer PCB. Although the circuit is quite complicated, by connecting several modules together, a large-scale solar simulator could be created.

The reduction of LEDs from 100 to 10 can increase their electrical power. Moreover, increasing the LED module's size will decrease the irradiance and increase the nonuniformity values beyond the IEC 60604-9 standard ranges. If the nonuniformity value can be maintained within the standard range, the irradiance obtained by the solar simulator will be less than 1 Sun. To test the PV characteristics, one can measure the voltage (V) and current (I) with the given irradiance, then determine the calibration factor to multiply by the V and I. In this way, the I-V characteristic of the PV module can be estimated, and, further, these values can be determined within the nonstandard test condition (non-STC). The advantage of this method is that it eliminates the need to build a large solar simulator that could produce 1 Sun of irradiance, thereby successfully reducing the LED module's electrical energy consumption.

The authors proposed to reduce the complicated factors such as the design, assembly, and control technique of the large-scale LED-based solar simulator (LLSS) and examine the calibration factor for spectral correction and application for PV characterization.

The LED-based solar simulator that the authors proposed could produce a spectrum according to class A of IEC 60904-9 [1]. The design concept of the LED module was the modular system, which was simple and easy to assemble on a large scale. The goal of this research was to design and build LLSS using a combination of six-color LEDs to form an LED module, to perform performance tests, such as spectral match, non-uniformity, and radiation instability under IEC 60904-9 standard [1], and to apply the LLSS for testing the I-V characteristic of a mono-crystalline PV module under non-STC.

2. Material and Methods

2.1. Design Target and Method

(1) Six different LED colors were sufficient to achieve a class-A spectral rating.

(2) Design was conducted by estimating six central LED wavelengths according to the AM1.5G reference spectrum and weight irradiance by manually adjusting the forward current of LEDs.

(3) LED module was made using a PCB configuration of 30 cm × 40 cm loaded with nine super power LEDs.

(4) The thermal management of the LEDS was conducted using a thin fin heat sink with a cooling fan.

(5) LED power was controlled using a DC/DC converter.

(6) LED solar simulator was designed, assembled, and tested by following the spectral match [1].

(7) Assembly of 12 LED modules resulted in an upscale to a LLSS.

(8) The non-uniformity of irradiance and of a large scale solar simulator was tested under IEC 60904-9 [1] to find out the best uniformity and the average irradiance on the test plane and measured the distribution of the straight spectrum with a value equal to or close to the average irradiance.

(9) For temporal instability, the authors tested only long-term operations because the built control system did not support the flash-mode operation.

(10) The spectrum distribution from (8) led us to determine a calibration factor through the use of a spectral mismatch calculator provided by PV-Lighthouse [19].

(11) The I-V characteristic of the mono-crystalline PV module was tested using the calibration factor from (10).

2.2. Solar Simulator Standards

For the indoor case of the solar cell I-V characteristic test, this study referred to the IEC 60904-9 standard (Photovoltaic device - Part 9: Solar simulator performance requirements) [1]. This standard tests three criteria: (a) The Spectral Match (SM) to all intervals; (b) The Spatial Non-uniformity of Irradiance (S_{NE}); and (c) The Temporal Instability of Irradiance (T_{IE}). The IEC 60904-9 standard [1] identifies the solar simulator class-A as SM= 0.75 – 1.25 and S_{NE} and $T_{IE} \leq 2\%$; class B: SM= 0.6 – 1.4 and S_{NE} and $T_{IE} \leq 5\%$; class C: SM= 0.4 – 2.0 and S_{NE} and $T_{IE} \leq 10\%$. Spatial non-uniformity of irradiance in percentage is calculated according to Equation (1):

$$S_{NE}\,(\%) = \left(\frac{E_{Max} - E_{Min}}{E_{Max} + E_{Min}}\right) \times 100 \quad (1)$$

where E was the irradiance measured over a defined test plane area. Temporal instability of irradiance was calculated by using Equation (2).

$$T_{IE}\,(\%) = \left(\frac{E_{Max} - E_{Min}}{E_{Max} + E_{Min}}\right) \times 100 \quad (2)$$

The spectral match can be measured with a spectroradiometer in the range of 400-1100 nm. This should measure the irradiance in each wave range of the bandwidth of light. There are six bandwidths, namely 400–500 nm, 500–600 nm, 600–700 nm, 700–800 nm, 800–900 nm, and 900–1100 nm. The measurement data was analyzed with the specific software. The measured results would be compared with the standard value of AM 1.5 G in each wavelength band. The percentage of the spectral match could then be determined. The percentage of total irradiance defined in the global reference solar spectral irradiance distribution was given in IEC 60904-3 [1].

2.3. LED Module Design

To achieve the designated goals, the authors proposed an LED module consisting of six colors. The authors chose the peak wavelength of LED as close as possible to the central wavelength of each spectral range according to the standard IEC 60904-9 [1]. The green LED efficiency was lowest (0.42) compared to the efficiency of the blue (0.93) and red (0.81) LEDs, while the efficiency of the infra-red LED was around 0.77. Based on Kusuma et al.'s [20] findings, one solar simulator module consisted of nine 50 W chip-on-board LEDs covering the six specific wavelengths in the range of 400-1100 nm. There are two groups of LEDs: (1) an infra-red LED comprising one 100 W 730 nm, two 50 W 850 nm, and two 50 W 940 nm (Fig. 2b); and (2) a visible light LED 50 W with four ranges, including 1×450 nm, 2×525 nm, and 1×650 nm. The visible group (450 nm, 525 nm, 650 nm) controlled the forward voltage and current by using the separate set of the constant current buck convertors. The infra-red LEDs were controlled and driven by an individual constant current buck/boost convertor. Fig. 1(b) showed the design position of the LED module by balancing out the visible and infra-red spectrum LEDs. This made them balance when assembled the 12 modules for a LLSS. The trial and error method was used for adjusting the light intensity of the LED module. The manual adjustment of intensity was run by keeping the spectrum in range of the class-A spectrum until reaching the maximum total intensity.

The assembly model of a solar simulator prototype was shown in Fig. 1(a). The authors could adjust the forward current and voltage of the LED in the CC and CV modes to control the percentage of irradiance of the LED in each range until the spectrum match met the AM 1.5 G. The complete circuit block diagram of the control irradiance of the LED and driver was shown in Fig. 2. The DC/DC converter was provided to control the LED V_F and I_F. One of the 36 V 450 W DC switching power supplies was supplied to drive one module of the LED solar simulator prototype.

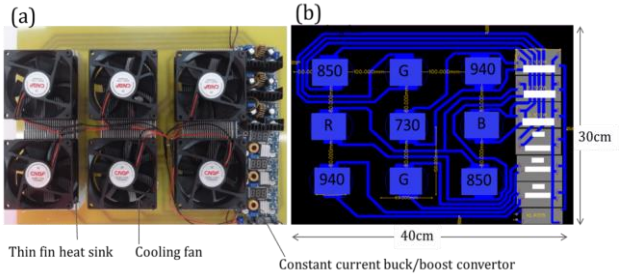

Fig. 1 Design of the LED solar simulator module with dimension 30 cm × 40 cm: (a) Prototype, (b) PCB design

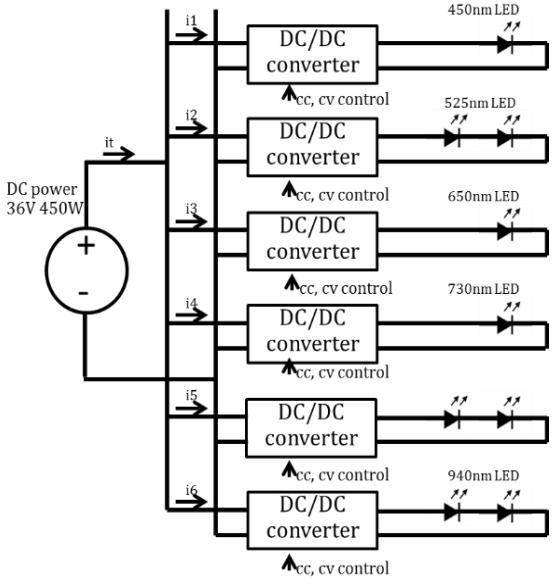

Fig. 2 The block diagram of the current control of the LED solar simulator's LED module

2.4. Large Scale LED-Based Solar Simulator

The structure of the LLSS was built using aluminum profiles. It was required to be large enough

to support a large PV module with the following dimensions: the outside was 140 cm × 200 cm × 150 cm, the test chamber was 125 cm × 190 cm × 60 cm, and the test plane was 96 cm × 152 cm. The test plane was fixed on two lifting columns with a range of 60 cm so that the test plane was positioned between 10 cm and 60 cm, as measured from the LED light modules. The LED irradiance was adjusted according to the difference between the test plane and the light source. Four sides of the test chamber were loaded with mirrors and supported with an aluminum frame for safety reasons and to increase the light uniformity on the test plane (Fig. 3). The roof of the LLSS comprised an aluminum frame with 12 LED modules and a cooling fan to remove the excess heat from inside the test chamber (Fig. 4). The 12 LED modules with 12 modules of 450 W / 220 V switching power supply distributed to balance the load for 3 phase 4 wire low voltage system. The irradiance was controlled by an up-down toggle switch. The PV panel characteristic test was controlled by a programmable electronics load, and the I-V measurement with a data logger was controlled via the personal computer.

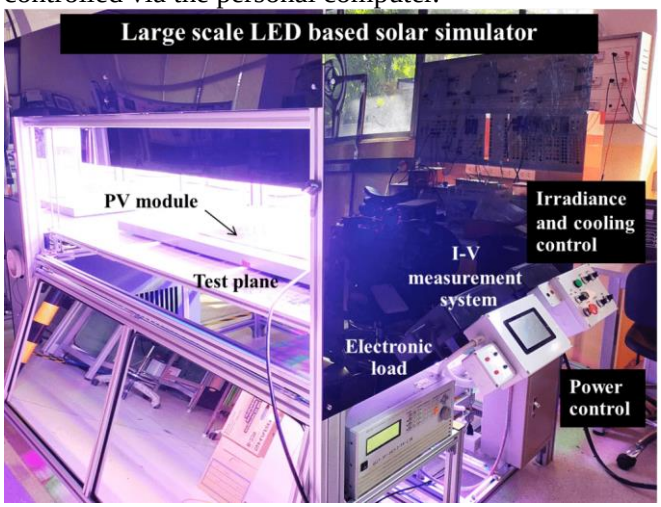

Fig. 3 The prototype of the LLSS

Fig. 4 Top view of the LED array under operation. D_L is the distance between the lighting areas of the LED module

2.5. Measurement

The Spectral match measurements were done by spectrometers calibrated by the National Institute of Metrology Thailand (NIMT). A Compact Array Spectrometer model: CAS140CT-154 was applied. The measured data were analyzed by the software Specwin-Pro. The measurement was carried out at the laboratory at an ambient temperature around 26°C and relative humidity of 60%.

The Spatial non-uniformity testing procedure was based on IEC-60904-9 Edition 2.0 2007-10 [1]. The test plane will be divided into 8 × 8 cells equally. The measurement will be taken three times and calculated for S_{NE} (Equation 1). The temporal instability of the solar simulator used for the testing procedure was based on the IEC 60904-9 [1]. The authors tested the long-term instability (LTI). The LTI in this study was tested for 10 minutes, and then, the information obtained was applied to calculate T_{IE} (Equation 2). To measure the irradiance was by the Class B Pyranometer (Kipp & Zonen).

The I-V characteristics of the 60 W (Ja-6120/18V) mono-crystalline PV module will be tested at a non-standard test condition. An electronics load (Model 63802, Chroma USA) and the custom I-V measurement system were applied for this experiment. The I-V characteristic curve of the PV panel under test was generated by spreadsheet software. The spectral calibration factor was determined by simulation on the software “Spectral Mismatch Calculator”.

3. Results and Discussion

3.1. Spectral Match Test

Table 1 showed the calculated spectral match in different wavelength intervals similar to Table 2 of IEC 60904-9 Edition 2.0 2007-10 with their associated expanded measurement uncertainties. The measurement was taken by 20 times per data set at 100 ms sampling time. The measurement results presented the spectral match as class A+ at all wavelength intervals (400 nm to 1100 nm). The spectral matches were within the range of 0.966-1.08 with a standard deviation less than ± 0.03 (Table 1). IEC norms declared the spectral mismatch below 12.5% (0.875 to 1.125) was a class A. Thus, from these results, the authors could claim that the spectral achieved class A+.

Table 1 Spectral match measurement results of the proposed LED module

Wavelength Interval	Percentage of Total Irradiance (% ± SD)	Spectral Match (Unit less ± SD)	Class
400 nm - 500 nm	17.9 ± 0.2	0.975 ± 0.012	A+
500 nm - 600 nm	19.8 ± 0.2	0.996 ± 0.010	A+
600 nm - 700 nm	18.6 ± 0.1	1.010 ± 0.010	A+
700 nm - 800 nm	14.8 ± 0.1	0.996 ± 0.008	A+
800 nm - 900 nm	13.5 ± 0.3	1.080 ± 0.030	A+
900 nm - 1100 nm	15.4 ± 0.1	0.966 ± 0.010	A+

This meant that the LED module that the authors proposed had shown a spectral match that highly resembled the AM 1.5 G standard spectral. The spectral intensity versus wavelength of the proposed spectrum was measured at the central point of a module, as shown in Fig. 5. The measured irradiance was 393.62 W/m^2 at 36.6 cm away from a LED module.

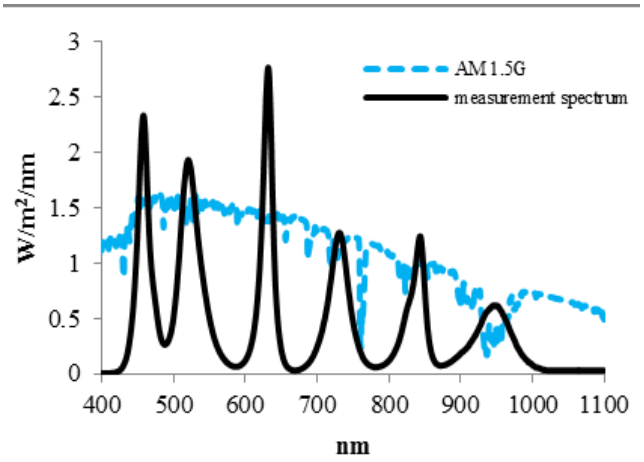

Fig. 5 Measurement results of the proposed spectrum compared to the AM 1.5G

The spectral distributions that the authors proposed were in class A+. This showed that the spectral mismatch was better than some previous studies. For example, the LED solar simulator had a variable flash speed and spectrum. The six-spectral LED-based solar simulator with irradiance control by LabVIEW was achieved in class B [8], [10]. However, the spectral mismatch of our LLSS had the same quality as the spectrum of a compact light-emitting diode-based class AAA that provided blue, red, far-red, infrared, and white (400 nm – 1100 nm) [4]. It was equivalent to the class AAA LED-based solar simulator for study-state and light soaking that provided twelve spectrums of LED on a wavelength range of 400 nm – 750 nm [9]. Ten different LED colors of a large area solar simulator achieved class AAA (wavelength 350 nm – 1100 nm) [18] and were able to obtain the same class as 32 LEDs with different wavelengths across the 350nm-1300nm range [21]. The spectral mismatch was important because it ensured that the test conditions matched to AM 1.5 G reference spectral and eliminated the variability from the batch-to-batch test [2].

The LED solar simulator provided the value of the spectral mismatch at class A. It was not dependent on the number of colors. Moreover, the number of spectrums should not be less than six and should cover wavelengths in the range of 400-1100 nm. However, a higher number of different LED spectrums will show a spectrum line that mimicked the solar spectrum and could reduce the error of the light intensity when compared to the AM1.5G spectrum.

3.2. Spatial Non-Uniformity of Irradiance (S_{NE}) Test

In the experiment, the authors adjusted the distance between the LED module and the test plane by using the irradiance control function of the solar simulator until the highest irradiance value was achieved, whose S_{NE} was not out of class C [1]. We found that the optimal distance (D_O) from the light source to the test plane was 44.1 cm. The measured results of the solar irradiance (W/m^2) from 64 measurement positions showed that the highest irradiance on the test plane was about 411 W/m^2 at position E6 of Fig. 6. The lowest is equal to 339 W/m^2 at positions A4 and A7. The average value of irradiance over the test plane was approximately 384 W/m^2 or 0.38 Sun. The calculation result of S_{NE} on the large test area of 152 cm × 96 cm (1.46 m^2) was equal to 9.60%, which met the IEC 60904-9 [1] in class-C.

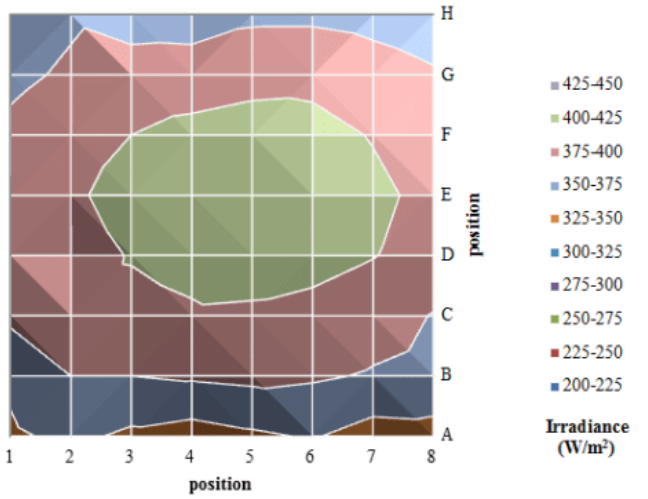

Fig. 6 The irradiance distribution on the test area in average irradiance was 384 W/m^2 at 44.1 cm distance from the light source

S_{NE} of this study was according to the large area solar simulator that used a metal halide lamp on a test area of 3.6 m^2 [22] and 1.8 m^2 [16] obtained in class C. This was similar to the uniformity of a LED solar simulator with variable flash speed and spectrum provided in class C of S_{NE} on a 100 mm × 100 mm area [11]. However, it was lower than the uniformity of the large area LED solar simulator designed by Al-Ahmad [18]. The LED solar simulator designed by Al-Ahmad [18] approached class A special non-uniformity of 1.99% with 4 LED modules of 32 cm × 9 cm in size connected to each other.

Comparing the S_{NE} obtained from this research to the S_{NE} from the small-scale solar simulator showed that the obtained S_{NE} was better. For instance, a compact light-emitting diode-based class AAA indicated that the S_{NE} met class A with a light area of 36 cm^2 [4]. The class AAA LED-based solar simulator for state study and light soaking that provided class A S_{NE} had a test area of about 324 cm^2 [9]. The class-A small area solar simulator (12 cm^2) for dye-sensitized solar cell testing was in class A S_{NE} by ASTM standard [2]. The LED solar simulator with a six-spectral wavelength across the 400 nm–1100 nm presented the SNE of less than 2% on the test plane of 910 cm^2 [10]. In addition, the LED-based solar simulator with an adjustable spectrum that proposed 23 different wavelengths of LED on the test area of 400 cm^2 also achieved the S_{NE} of Class A [23].

The small-scale solar simulator could provide good S_{NE} because the distance between the LEDs was too small, only about 12 to 22 mm [4], [9], which was due to the usage of the small LEDs package such as super-

flux or SMD (the diameter was around 6 to 10 mm). It made sense when the light generator was small, and the small LED should be selected. This was the cause of achieving good S_{NE}. On the other hand, in the case of LLSS, it was difficult to obtain the S_{NE} in class A.

However, the non-uniformity of the irradiance of the LLSS in this paper was not accepted in Classes A and B because the distance (D_L in Fig. 4) between the LED modules and the test area was quite far apart. The D_L was about 100 mm. The distance from the center to the center of the LEDs on a module was around 80–100 mm. For decreasing the percentage of S_{NE}, the distance of D_L had to be reduced.

From the results, a LLSS could generate an irradiance of about 0.38 Sun. While it was known that the irradiance of 0.38 Sun could be used to characterize the PV module, it cannot be used on the standard test condition (STC). Usually, an irradiance of 1 Sun is required for STC. To increase the irradiance, the authors had to increase the LED power and the number of LEDs module. Even though the number of LEDs increased, the percentage of irradiance in the range of 400–1100 nm was still the same as the original design, confirming that the spectral mismatch was as close as class A. This would be the point for the author to improve in the next study

3.3. Temporal Instability of Irradiance (T_{IE}) Test

This section included the results of the T_{IE} test under long-term stability (LTI), executed while the solar simulator was run for 10 min. An irradiance sensor was placed on the center of the test plane and 44.1 cm from the light source. Measurement was taken in three rounds, and from that, the average irradiance was found (E_{Max} = 399.20 W/m^2 and E_{Min} = 395.50 W/m^2). Lastly, T_{IE} was calculated under IEC 60904-9 [1]. For setting up the experiment, the warm-up time was 60 s, and the sampling time was about 2 s, as shown in Fig. 7. The calculated T_{IE} was equal to 0.76%, met the class A+ standard (class A is < 2%, class A+ is < 1%). Another factor was to maintain the T_{IE} in good condition as the operating temperature of LED modules and using optimal cooling methods such as an active cooling device.

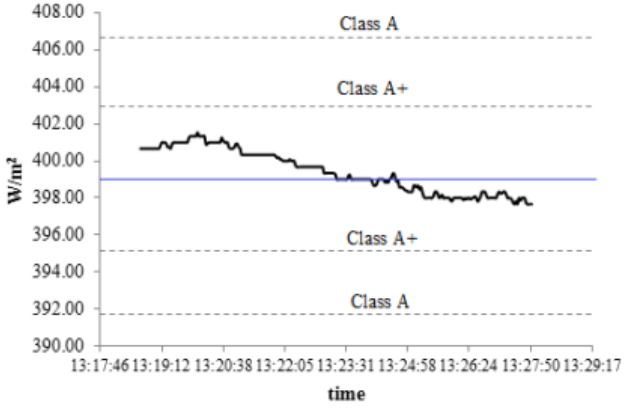

Fig. 7 Irradiance vs. time of the testing of LLSS for LTI determination (warm-up time - 60 s). T_{IE} is indicated in class A+

The obtained T_{IE} was a value of 0.76%, which corresponded to Class A+, and in accordance with the T_{IE} of LED large scale solar simulator provided by Al-Ahmad et al. (0.31%, class A$^+$) [18]. This was not different from the T_{IE} of a low-cost LED-based solar simulator after a 60 s warm-up, 0.4582% (Class A$^+$) [7]. Similarly, the T_{IE} of compact light-emitting diode class AAA solar simulator after several minutes of warm-up time was less than 0.25% (class A$^+$) [4]. From the previous studies [4], [7], [15], [18], it was provided that the aluminum heat sink with a cooling fan could serve as the LED's cooling system, so it resulted in the T_{IE} meeting the class A$^+$. However, if a water-cooled height-adjustable aluminum block was used as an LED cooling system, T_{IE} < 0.1% [9]. In addition, the LED flash solar simulator [11] could provide T_{IE} < 0.1% because the LED was operated in a short time, which influenced the temperature of LED to be lower than long time operation, resulting in a quite stable temporal stability.

In summary, the performance of the LLSS that the authors proposed could meet Classes A$^+$, C, and A$^+$. The spectral mismatch was in class A$^+$. The non-uniformity of irradiance was in class C, and temporal instability was in class A+.

3.4. Calibration Factor

Since the irradiance of the proposed spectrum was not equal to 1 Sun (1000 W/m^2), the authors had to determine the calibration factor by using a Spectral Mismatch Calculator. It was used for determining the PV module characterization under non-STC. The proposed spectrum was measured from Position B5 (Fig. 6). The authors measured the spectrum at this point because the irradiance was close to the average irradiance on the test plane. The authors called this spectrum 0.38 Sun. It was shown in Fig. 9 as a red dot line from experimental results. The spectral intensity of the AM 1.5 G spectra was loaded from the spectrum library (Fig. 9, AM 1.5 G as an orange line) of the Spectral Mismatch Calculator. The AM 1.5 G was set; the total intensity was 100 mW/cm^2. Setting up the spectrum was in the range of 400–1100 nm. The authors had to define the calibration factor by multiplying the spectral intensity of the proposed spectrum until the short circuit current of the solar cell specimen under the proposed spectrum was equal to under AM 1.5 G. This study proposed the WPVS reference cell (World PV Scale Standard; mono-crystalline silicon solar cell) as a specimen because WPVS is recognized as an international standard for calibrating reference cells used in the characterization of solar cells and modules [24]. The procedure to determine the calibration factor and I-V characteristic under non-STC was shown in detail in Fig. 8. The simulated spectral result after calibration is shown in Fig. 9.

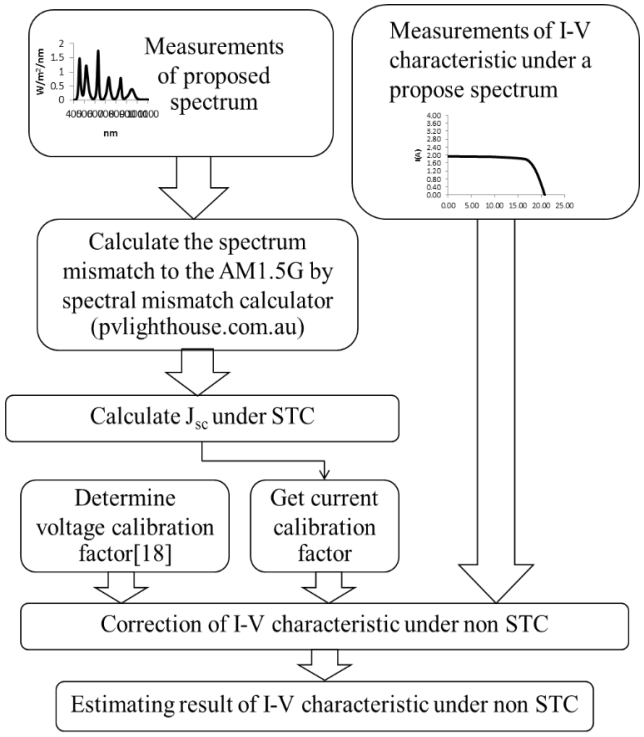

Fig. 8 Procedure for determining an I-V characteristic under non-STC in this study

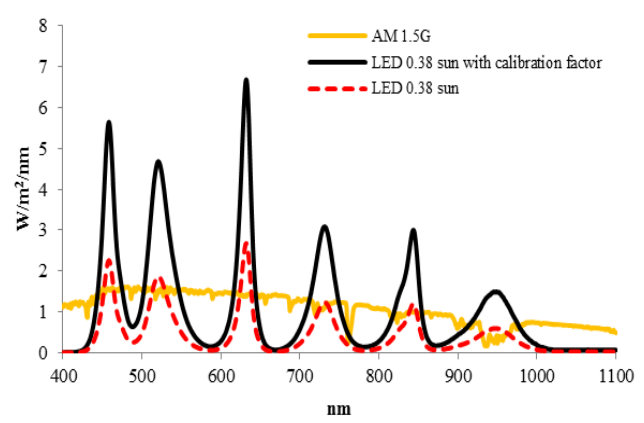

Fig. 9 Comparison of the proposed spectral (LED 0.38 Sun), AM 1.5 G spectral and proposed spectral after calibration (LED 0.38 Sun with calibration factor)

In the Spectral Mismatch Calculator, the authors increased the scaling factor of the proposed spectrum until the short-circuit current density (J_{SC}) of the solar cell specimen was equal to the J_{SC} under AM 1.5 G spectral at 33.33 mA/cm². In this case, the scaling factor was equal to 251.16%. Therefore, we can say that the current calibration factor was equal to 2.512. It was used for multiplying the measured current of the PV module under LED 0.38 Sun. The proposed spectral after calibration is shown in Fig. 9.

In the case of PV voltage, V_{oc} was increased slightly logarithmically when irradiation value had increased. From the research of Khan et al. [25], the study reported between V_{oc} and irradiance, when experimenting with mono-crystalline solar cells (size 8 cm^2), V_{oc} increased by 107.472% when irradiance increased from 380 W/m^2 to 1000 W/m^2. Therefore, the authors applied the 1.0747 multiply to the PV voltage in this study, namely a voltage calibration factor.

The I-V characteristic tested under the LED 0.38 Sun multiplied the PV current by 2.512, without multiplying the PV voltage factor by 1.0747. Therefore, after multiplying by the calibration factor, the PV characteristic was likely close to testing under 1000 W/m^2 of the standard test condition [26], as shown in Fig. 10.

3.5. PV Module Characterizations under LLSS

A prototype of LLSS was applied to test the I-V characteristic of a 60 W mono-crystalline PV module under non-STC. The average irradiance on the test area was 384 W/m^2 or 0.38 Sun (the spectral match in class A+), with the PV module connected to the electronics load. The load was programmed to increase 0.1A per step at a maximum current of 3.5 A. The temperature of the PV module was 25 ± 3°C. The load current and voltage of a PV module were recorded by the measurement system of electronic load and plotted by the spreadsheet software. The obtained I-V characteristic curves were applied before and after calibration as shown in Fig. 10(a) and (b). The red line in Fig. 10 showed the I-V and P-V characteristics after multiplication by the calibration factor.

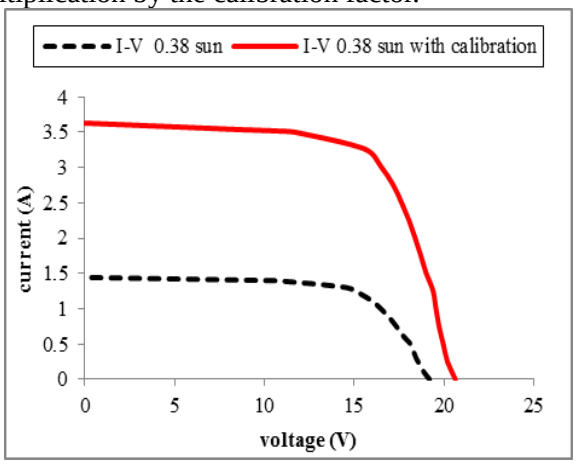

(a)

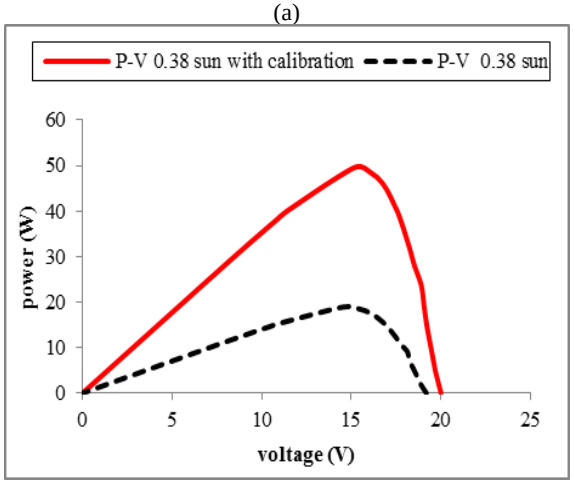

(b)

Fig. 10 (a) The measurements of I-V curve of 60 W PV module tested on LED solar simulator under 0.38 Sun with and without the calibration factor and (b) P-V curve of 60 W PV module with and without the calibration

From Fig. 10(b), we can read the PV characteristics such as open-circuit voltage (V_{OC}), short-circuit current (I_{SC}), maximum power (P_{max}), maximum power voltage (V_{pmax}), and maximum power current (I_{pmax}) from the measurements and compare them with those provided by the manufacturer's nameplate as in Table 2. The comparative results found that the trend of voltage and current characteristic of the PV module under LLSS (class A+ C A+) after calibration was consistent with the manufacturer's data. Table 2 indicates that the measured PV current had extremely small relative errors from the nameplate current at about 2.44% to 4.81% when estimating with the calibration factor. The PV voltage after the calibration factor was estimated with V_{oc} and V_{pmax} values of 3.21% and 11.01%, respectively.

Table 2 The I-V characteristic of 60 W mono-crystalline PV module from measurement with calibration and voltage factors

Photovoltaic characteristic	Typical (nameplate)	Measurement with calibration	Error (%)
Open-circuit voltage (V_{OC})	21.32	20.63	3.21
Short-circuit current (I_{SC})	3.72	3.63	2.44
Maximum power (P_{max})	60.00	50.85	15.26
Maximum power voltage (V_{pmax})	17.50	15.57	11.01
Maximum power current (I_{pmax})	3.43	3.27	4.81

Here, the error between measuring and typical data should be caused by poor uniformity. Our LLSS provided the S_{NE} in class C, resulting in a short-circuit current lower than the nameplate current at about 2.44%. Increasing nonuniformity may have affected the decrease in the photo current and short-circuit current (I_{SC}) of a PV module. Nonuniformity was probably the most difficult specification to achieve, especially for large-area solar simulator. If uniformity was increased, it could decrease solar cell performance testing and repeatability [2]. According to the study of Herrmann and Wiesner [27], increasing the nonuniformity of irradiance mainly affected the short-circuit current and Fill factor (FF). The I_{SC} was underrated and FF consequently overrated. The open circuit voltage still unaffected the non-uniformity. Song et al. [28] reported the effect of non-uniform irradiance on module performance and confirmed that the maximum power and short circuit current of the PV module without a bypass diode will decrease when the non-uniformity increases.

The error of V_{OC} was around 3.21% when analyzing the voltage parameters of the PV module, which was accepted. However, the V_{pmax} from the measurement compared to the name plate was 11.01% of error. An error of V_{pmax} could occur for the following reasons. For example, the voltage factor used in this study was not derived from the PV module used in this study. Another point was that the efficiency of the PV module used may differ from the solar cell efficiency used in the study by Khan et al. [25], even if it was the same mono crystalline type.

In sum, the calibration factor was comprised of the current factor and the voltage factor. The current factor was received from simulation by the Spectral Mismatch Calculator [19] and the voltage factor was determined by Khan et al. [25]. The calibration factor was an alternative way to estimate the I-V characteristic curve of the PV module under non STC. The calibration factor from this study was applied for the I-V characterization of the mono crystalline module under LED solar simulator at 0.38 Sun. It could not be used for testing the electrical features of other types of solar cells, such as a-Si, GIC, and so on.

4. Conclusion

The authors suggested the novel idea to achieve the LED modular system that could be extended as a large-scale solar simulator. The 96 cm × 152 cm of LLSS could be easily assembled using twelve LED modules. The six spectral of the LED could attain a class A^+ spectral match and a class A^+ instability due to the efficient cooling system of LED module. The non-uniformity of irradiance was in class C. The poor non-uniformity of the solar simulator resulted in a reduction in the short circuit current of the PV module that tested under non-STC. The I-V characteristics of the mono crystalline PV module were tested by the solar simulator prototype, producing values as close to those as in the typical data sheet. The I-V characteristics under non-STC could be estimated by finding out the calibration factor. However, this novel principle may apply to PV module testing with solar simulator under low radiation condition. Similarly, if a PV module is tested under STC, the LED module must produce light intensity of 1000 W/m^2, which must be redesigned with the increased power of LED and symmetrical alignment. This will then increase the power consumption of the LED module by approximately three times. This approach, presented by the researchers, is interesting and practical.

The modular type of LED light sources that the authors proposed could reduce the complications of the LLSS prototype, such as the light sources design, the stack of DC power supplies design, hardware assembly, thermal management, and control techniques of the large-scale LED-based solar simulator.

The experimental results were limited to a mono-crystalline solar cell. Therefore, they do not confirm that this simple calibration factor technique will work well for other types of solar panels.

For further research, the LED module should be developed to meet the class A non-uniformity of solar simulator prototype according to IEC 60904-9 [1].

Acknowledgments

The authors would like to credit the PV education webpage, which provides a powerful spectral mismatch calculator for this study. Next, we would like to thank the National Research Council of Thailand, which provided the research budget. Lastly, we give many thanks to Ms. Pattaraporn Watjanatepin for proofing the writing of this paper.

References

[1] INTERNATIONAL ELECTROTECHNICAL COMMISSION. *IEC 60904-9: Photovoltaic devices — Part 9: Solar simulator performance requirements*, 2007. https://webstore.iec.ch/preview/info_iec60904-9%7Bed2.0%7Db.pdf

[2] SALAM R. A., SAPUTRA C., and YULIZA E. Development of a simple low-scale solar simulator and its light distribution. Proceedings of the International Conference on Instrumentation, Control and Automation, Bandung, 2016, pp. 28–31. https://doi.org/10.1109/ICA.2016.7811470

[3] FROLOVA T. I., CHURYUMOV G. I., VLASYUK V. M., and KOSTYLYOV V. P. Combined Solar Simulator for Testing Photovoltaic Devices. Proceedings of the 1st Global Power, Energy and Communication Conference, Nevsehir, 2019, pp. 276-280. https://doi.org/10.1109/GPECOM.2019.8778607

[4] NOVICKOVAS A., BAGUCKIS A., MEKYS A., and TAMOŠIŪNAS V. Compact light-emitting diode-based AAA Class solar simulator: design and application peculiarities. *IEEE Journal of Photovoltaics*, 2015, 5(4): 1137–1142. https://doi.org/10.1109/JPHOTOV.2015.2430013

[5] TAVAKOLI M., JAHANTIGH F., and ZAROOKIAN H. Adjustable high-power-LED solar simulator with extended spectrum in UV region. *Solar Energy*, 2021, 220: 1130-1136. https://doi.org/10.1016/j.solener.2020.05.081

[6] ESEN V., SAGLAM S., ORAL B., and ESEN O. C. Spectrum measurement of variable irradiance controlled LED-based solar simulator. *International Journal of Renewable Energy Research*, 2020, 10(1): 109-116. https://ijrer.org/ijrer/index.php/ijrer/article/view/10335

[7] LÓPEZ-FRAGUAS E., SÁNCHEZ-PENA J. M., and VERGAZ R. A low-cost LED-based solar simulator. *IEEE Transactions on Instrumentation and Measurement*, 2019, 68(12): 4913-4923. https://doi.org/10.1109/TIM.2019.2899513

[8] BLISS M., BETTS T. R., and GOTTSCHALG R. Initial solar cell characterisation test and comparison with a LED-based solar simulator with variable flash speed and spectrum. Proceedings of the Photovoltaic Science Application and Technology Conference, Bath, 2008, pp. 215-218.

[9] STUCKELBERGER M., PERRUCHE B., BONNET-EYMARD M., RIESEN Y., DESPEISSE M., HAUG F.-J., and BALLIF C. Class AAA LED-based solar simulator for steady-state measurements and light soaking. *IEEE Journal of Photovoltaics*, 2014, 4(5): 1282–1287. https://doi.org/10.1109/JPHOTOV.2014.2335738

[10] WATJANATEPIN N. Design construct and evaluation of six-spectral LEDs-based solar simulator based on IEC 60904-9. *International Journal of Engineering and Technology*, 2017, 9(2): 923-931. https://doi.org/10.21817/ijet/2017/v9i2/170902101

[11] RUMYANTSEV V. D., LARIONOV V. R., MALEVSKIY D. A., POKROVSKIY P. V., and SADCHIKOV N. A. Solar simulator for characterization of the large-area HCPV modules. *AIP Conference Proceedings*, 2011, 1407: 212. https://doi.org/10.1063/1.3658329

[12] CHEN Q., JIN X., and XUE L. Modeling and optimization of multi-LED solar spectrum synthesis with widely-tuning radiant flux output. *Optik*, 2019, 180: 276-284. https://doi.org/10.1016/j.ijleo.2018.11.102

[13] ALDOSHINA O., YUGAY V., KALIASKAROV N., ESENJOLOV U., and NESIPOVA S. Solar simulator on the basis of powerful light-emitting diodes. *MATEC Web of Conferences*, 2018, 155: 01035. https://doi.org/10.1051/matecconf/201815501035

[14] CABALLERO C. A. U., PONCE R. R., and MUÑOZ F. G. M. Design of a LED-based solar simulator for energy harvesting applications. Proceedings of the IEEE International Autumn Meeting on Power, Electronics and Computing, Ixtapa, 2017, pp. 1-6. https://doi.org/10.1109/ROPEC.2017.8261661

[15] BODNÁR I., KOÓS D., ISKI P., and SKRIBANEK Á. Design and Construction of a Sun Simulator for Laboratory Testing of Solar Cells. *Acta Polytechnica Hungarica*, 2020, 17(3): 165-184. https://doi.org/10.12700/aph.17.3.2020.3.9

[16] COLAROSSI D., TAGLIOLINI E., PRINCIPI P., and FIORETTI R. Design and Validation of an Adjustable Large-Scale Solar Simulator. *Applied Sciences*, 2021, 11(4): 1964. https://doi.org/10.3390/app11041964

[17] MENG Q., WANG Y., and ZHANG L. Irradiance characteristics and optimization design of a large-scale solar simulator. *Solar Energy*, 2011, 85(9): 1758-1767. https://doi.org/10.1016/j.solener.2011.04.014

[18] AL-AHMAD A. Y., VAUGHAN B., HOLDSWORTH J., ZHOU X., BELCHER W., and DASTOOR P. LED Configuration for Large Area Solar Simulator Applications. Proceedings of the International Conference on Nanoscience and Nanotechnology, Wollongong, 2018. https://www.researchgate.net/publication/322909851_LED_Configuration_for_Large_Area_Solar_Simulator_Applications

[19] PV LIGHTHOUSE. *Spectral Mismatch Calculator*, n.d. https://www.pvlighthouse.com.au/

[20] KUSUMA P., PATTISON P. M., and BUGBEE B. From physics to fixtures to food: current and potential LED efficiency. *Horticulture Research*, 2020, 7(56): 1-9. https://doi.org/10.1038/s41438-020-0283-7

[21] PLYTA F., BETTS T., and GOTTSCHALG R. Potential for LED solar simulators. Proceedings of the IEEE 39th Photovoltaic Specialists Conference, Tampa, Florida, 2013, pp. 0701-0705. https://doi.org/10.1109/PVSC2013.6744248

[22] MATIAS C. A., FURRIEL G. P., SANTOS L. M., CALIXTO W. P., BARBOSA J. L. F., DE OLIVEIRA S. B., and ALVES A. J. Optimized Solar Simulator Structure for Uniform Irradiance Distribution. Proceedings of the IEEE International Conference on Environment and Electrical Engineering and IEEE Industrial and Commercial Power Systems Europe, Palermo, 2018, pp. 1-6. https://doi.org/10.1109/EEEIC.2018.8494430

[23] LINDEN K. J., NEAL W. R., and SERREZE H. B. Adjustable spectrum LED solar simulator. Proceedings

Volume 9003, Light-Emitting Diodes: Materials, Devices, and Applications for Solid State Lighting XVIII, 2014, 900317. https://doi.org/10.1117/12.2035649
[24] OSTERWALD C. R., ANEVSKY S., BARUA A. K., CHAUDHURI P., DUBARD J., EMERY K., HANSEN B., KING D., METZDORF J., NAGAMINE F., SHIMOKAWA R., WANG Y.X., WITTCHEN T., ZAAIMAN W., ZASTROW A., and ZHANG J. The World Photovoltaic Scale: An International Reference Cell Calibration Program. Proceedings of the 26th IEEE Photovoltaic Specialists Conference, Anaheim, California, 1997, pp. 1209-1212. https://doi.org/10.1109/PVSC.1997.654306
[25] KHAN F., SINGH S. N., and HUSAIN M. Effect of illumination intensity on cell parameters of a silicon solar cell. *Solar Energy Materials and Solar Cells*, 2010, 94(9): 1473-1476. https://doi.org/10.1016/j.solmat.2010 .03.018
[26] DIRNBERGER D. Photovoltaic module measurement and characterization in the laboratory. In: PEARSALL N. (ed.) *The Performance of Photovoltaic (PV) Systems: Modelling, Measurement and Assessment*. Woodhead Publishing, Cambridge, 2017: 23-70. https://doi.org/10.1016/B978-1-78242-336-2.00002-1
[27] HERRMANN W., & WIESNER W. Modeling of PV Modules - The Effects of Non-Uniform Irradiance on Performance Measurements with Solar Simulators. Proceedings of the 16th European Photovoltaic Solar Energy Conference, Glasgow, 2000. https://doi.org/10.4324/9781315074405-71
[28] SONG T., JOHNSTON S., FRÜHAUF F., BAUER J., BREITENSTEIN O., and LEVI D. Quantitative Study of the Effect of Non-Uniform Irradiance on Module Performance Combining EL and DLIT Imaging with Circuit Modeling. Proceedings of the IEEE 7th World Conference on Photovoltaic Energy Conversion, Waikoloa Village, Hawaii, 2018, pp. 3618-3622. https://doi.org/10.1109/PVSC.2018.8548278
[29] JAPANESE STANDARDS ASSOCIATION. *JIS C 8912: Solar Simulators for Crystalline Solar Cells and Modules*, 2015. https://global.ihs.com/doc_detail.cfm?document_name=JIS%20C%208912&item_s_key=00275485
[30] ASTM INTERNATIONAL. *ASTM E927-05: Standard Specification for Solar Simulation for Terrestrial Photovoltaic Testing.* ASTM International, West Conshohocken, Pennsylvania, 2005. https://doi.org/10.1520/E0927-05

参考文:

[1] 国际电工委员会。国际电工委员会60904-9：光伏设备 — 第 9 部分：太阳能模拟器性能要求，2007。https://webstore.iec.ch/preview/info_iec60904-9%7Bed2.0%7Db.pdf
[2] SALAM R. A.、SAPUTRA C. 和 YULIZA E. **开**发一个简单的低尺度太阳模拟器及其光分布。仪表、控制和自动化国际会议论文集，万隆，2016，第 28-31 页。https://doi.org/10.1109/ICA.2016.7811470
[3] FROLOVA T. I.、CHURYUMOV G. I.、VLASYUK V. M. 和 KOSTYLYOV V. P. 用于测试光伏设备的组合太阳能模拟器。第一届全球电力、能源和通信会议论文集，内夫谢希尔，2019，第 276-280 页。https://doi.org/10.1109/GPECOM.2019.8778607
[4] NOVICKOVAS A.、BAGUCKIS A.、MEKYS A. 和 TAMOŠIŪNAS V. 基于紧凑型发光二极管的 AAA 级太阳能模拟器：设计和应用特性。IEEE 光伏杂志，2015，5(4)：1137–1142。https://doi.org/10.1109/JPHOTOV.2015.2430013
[5] TAVAKOLI M.、JAHANTIGH F. 和 ZAROOKIAN H. 可调节的高功率引领太阳模拟器，在紫外线区域具有扩展光谱。太阳能，2021，220：1130-1136。https://doi.org/10.1016/j.solener.2020.05.081
[6] ESEN V.、SAGLAM S.、ORAL B. 和 ESEN O. C. 可变辐照度控制的基于引领的太阳模拟器的光谱测量。国际可再生能源研究杂志，2020，10(1)：109-116。https://ijrer.org/ijrer/index.php/ijrer/article/view/10335
[7] LÓPEZ-FRAGUAS E.、SÁNCHEZ-PENA J. M. 和 VERGAZ R. 一**种**基于引领的低成本太阳能模拟器。IEEE 仪器与测量汇刊，2019，68(12)：4913-4923。https://doi.org/10.1109/TIM.2019.2899513
[8] BLISS M.、BETTS T. R. 和 GOTTSCHALG R. 初始太阳能电池特性测试以及与具有可变闪光速度和光谱的基于引领的太阳能模拟器的比较。光伏科学应用与技术会议论文集，巴斯，2008，第 215-218 页。
[9] STUCKELBERGER M., PERRUCHE B., BONNET-EYMARD M., RIESEN Y., DESPEISSE M., HAUG F.-J. 和 BALLIF C. 基于 AAA 级引领的太阳能模拟器，用于稳态测量和光吸收。IEEE 光伏杂志，2014，4(5)：1282–1287。https://doi.org/10.1109/JPHOTOV.2014.2335738
[10] WATJANATEPIN N. 基于国际电工委员会60904-9的基于六光谱引领的太阳能模拟器的设计构造和评估。国际工程技术杂志，2017，9(2)：923-931. https://doi.org/10.21817/ijet/2017/v9i2/170902101
[11] RUMYANTSEV V. D.、LARIONOV V. R.、MALEVSKIY D. A.、POKROVSKIY P. V. 和 SADCHIKOV N. A. 用于表征大面积丙型肝炎病毒模块的太阳能模拟器。AIP 会议论文集，2011，1407：212。https://doi.org/10.1063/1.3658329
[12] CHEN Q., JIN X., 和XUE L. 具有广泛调谐辐射通量输出的多引领太阳光谱合成的建模和优化。光学，2019，180：276-284。https://doi.org/10.1016/j.ijleo.2018.11.102
[13] ALDOSHINA O.、YUGAY V.、KALIASKAROV N.、ESENJOLOV U. 和 NESIPOVA S. 基于强大发光二极管的太阳能模拟器。马泰克会议网络，2018，155：01035. https://doi.org/10.1051/matecconf/201815501035
[14] CABALLERO C. A. U.、PONCE R. R. 和 MUÑOZ F. G. M. 用于能量收集应用的基于引领的太阳能模拟器的设计。IEEE 国际电力、电子和计算秋季会议论文集，伊斯塔帕，2017，第 1-6 页。https://doi.org/10.1109/ROPEC.2017.8261661
[15] BODNÁR I.、KOÓS D.、ISKI P. 和 SKRIBANEK Á. 用于太阳能电池实验室测试的太阳模拟器的设计和构造。匈牙利理工学院学报，2020，17(3)：165-184。https://doi.org/10.12700/aph.17.3.2020.3.9
[16] COLAROSSI D.、TAGLIOLINI E.、PRINCIPI P. 和 FIORETTI R. 可调节大型太阳模拟器的设计和验证。应用科学，2021，11(4)：1964. https://doi.org/10.3390/app11041964

[17] MENG Q., WANG Y., 和ZHANG L. 大型太阳模拟器的辐照度特性和优化设计。太阳能，2011，85(9)：1758-1767。https://doi.org/10.1016/j.solener.2011.04.014
[18] AL-AHMAD A. Y.、VAUGHAN B.、HOLDSWORTH J.、ZHOU X.、BELCHER W. 和 DASTOOR P. 大面积太阳能模拟器应用的引领配置。国际纳米科学与纳米技术会议论文集，卧龙岗，2018。https://www.researchgate.net/publication/322909851_LED_Configuration_for_Large_Area_Solar_Simulator_Applications
[19] 光伏灯塔。光谱失配计算器，未注明日期。https://www.pvlighthouse.com.au/
[20] KUSUMA P.、PATTISON P. M. 和 BUGBEE B. 从物理学到固定装置再到食物：当前和潜在的引领效率。园艺研究，2020，7(56)：1-9. https://doi.org/10.1038/s41438-020-0283-7
[21] PLYTA F.、BETTS T. 和 GOTTSCHALG R. 引领太阳能模拟器的潜力。IEEE 第 39 届光伏专家会议论文集，佛罗里达州坦帕，2013，第 0701-0705 页。https://doi.org/10.1109/PVSC2013.6744248
[22] MATIAS C. A.、FURRIEL G. P.、SANTOS L. M.、CALIXTO W. P.、BARBOSA J. L. F.、DE OLIVEIRA S. B. 和 ALVES A. J. 用于均匀辐照度分布的优化太阳模拟器结构。IEEE 环境与电气工程国际会议和 IEEE 欧洲工业和商业电力系统会议论文集，巴勒莫，2018，第 1-6 页。 https://doi.org/10.1109/EEEIC.2018.8494430
[23] LINDEN K. J.、NEAL W. R. 和 SERREZE H. B. 可调光谱引领太阳模拟器。论文集第 9003 卷，发光二极管：固态照明的材料、器件和应用 XVIII，2014，900317。https://doi.org/10.1117/12.2035649
[24] OSTERWALD C. R., ANEVSKY S., BARUA A. K., CHAUDHURI P., DUBARD J., EMERY K., HANSEN B., KING D., METZDORF J., NAGAMINE F., SHIMOKAWA R., WANG Y. X., WITTCHEN T., ZAAIMAN W., ZASTROW A., 和ZHANG J. 世界光伏规模：国际参考电池校准计划. 第 26 届 IEEE 光伏专家会议论文集，加利福尼亚州阿纳海姆，1997，第 1209-1212 页。https://doi.org/10.1109/PVSC.1997.654306
[25] KHAN F.、SINGH S. N. 和 HUSAIN M. 光照强度对硅太阳能电池的电池参数的影响。太阳能材料与太阳能电池，2010，94(9)：1473-1476。https://doi.org/10.1016/j.solmat.2010 .03.018
[26] DIRNBERGER D. 实验室中的光伏组件测量和表征。在：PEARSALL N. (编。) 光伏 (光伏) 系统的性能：建模、测量和评估。伍德黑德出版社，剑桥，2017：23-70。 https://doi.org/10.1016/B978-1-78242-336-2.00002-1
[27] HERRMANN W., & WIESNER W. 光伏模块建模 - 非均匀辐照度对太阳能模拟器性能测量的影响。第 16 届欧洲光伏太阳能会议论文集，格拉斯哥，2000。https://doi.org/10.4324/9781315074405-71
[28] SONG T.、JOHNSTON S.、FRÜHAUF F.、BAUER J.、BREITENSTEIN O. 和 LEVI D. 将 EL 和 DLIT 成像与电路建模相结合的非均匀辐照度对模块性能影响的定量研究。IEEE 第七届世界光伏能源转换会议论文集，夏威夷威可洛亚村，2018 年，第 3618-3622 页。https://doi.org/10.1109/PVSC.2018.8548278
[29] 日本标准协会。日本工业标准C 8912：晶体太阳能电池和组件的太阳能模拟器，2015。https://global.ihs.com/doc_detail.cfm?document_name=JIS%20C%208912&item_s_key=00275485
[30] ASTM 国际。ASTM E927-05：用于地面光伏测试的太阳模拟标准规范。ASTM国际，宾夕法尼亚州西康绍霍肯，2005。https://doi.org/10.1520/E0927-05